Chinese Herbal Medicines 11 (2019) 200–208

Contents lists available at ScienceDirect

Chinese Herbal Medicines

journal homepage: www.elsevier.com/locate/chmed

Original Article

Discrimination of toxic ingredient between raw and processed *Pinellia ternata* by UPLC/Q-TOF-MS/MS with principal component analysis and T-test

Xing-ying Zhai, Ling Zhang, Bing-tao Li, Yu-lin Feng, Guo-liang Xu, Hui Ouyang, Shi-lin Yang, Chen Jin*

Jiangxi University of Traditional Chinese Medicine, Nanchang 330004, China

ARTICLE INFO

Article history:
Received 25 May 2018
Revised 15 August 2018
Accepted 5 November 2018
Available online 21 March 2019

Keywords:
discrimination
principal component analysis
raw and processed *Pinellia ternata* (Thunb.) Berit.
toxic ingredient
T-test
UPLC/Q-TOF-MS/MS

ABSTRACT

Objective: To investigate the toxicity difference between raw and processed *Pinelliae Rhizoma* (Banxia in Chinese, BX), the rhizoma of *Pinellia ternata*, from the view of chemical composition.
Methods: Sixteen samples of raw and processed BX were prepared and analyzed by UPLC/Q-TOF-MS/MS. The discrimination (chemical marker) between the two group was investigated by principal component analysis (PCA) and T-test analysis. According to the accurate charge-to-mass ratio, MS/MS fragments, and comparison of corresponding data with the reference or database, the chemical markers were identified preliminarily.
Results: Liquiritin, liquiritigenin, and lysophosphatidylcholine (LPC) were identified as the characteristic markers. The reducing of LPC in processed BX was one of the main reasons for detoxification because LPC could induce the inflammatory response; Liquiritin and liquiritigenin showed the anti-inflammatory effect and reduced liver injury, therefore the appearance of them in processed BX was an another reason for detoxification.
Conclusion: An approach to explain the mechanisms of reducing the toxicity in medicinal plants by processing was proposed. Moreover, the chemical markers of toxicity could be used to differentiate the raw material from processed herbs for the quality control and safety application in clinical practice.

1. Introduction

In the theories of traditional Chinese medicine, the processing of traditional Chinese herbs is a common practice. Herbs are usually processed for increasing efficacy and/or decreasing toxicities and side effects (Jin & Wang, 2004). It has been proved that the processing procedure could reduce the toxicity (Ye & Yuan, 2005).

Pinelliae Rhizoma (Banxia in Chinese, BX), the rhizoma of *Pinellia ternata* (Thunb.) Berit., is a valuable Chinese materia medica for its therapeutic effect to treat the cough, vomiting, infection, and inflammation related diseases. However, raw BX (RBX) may cause adverse effects such as tongue numbing, tongue swelling, salivary secretion, slurring of speech, and hoarseness. The previous study indicated that excessive or long-term use of RBX could cause liver and kidney damage (Yang, Ye, & Wu, 1988; Zhang, Huang, & Bao, 2011). RBX may possess certain cardiotoxicity in SD rats (Zhang et al., 2013). The high dosage of RBX extracts might lead to fetal malformation in the pregnant Sprague Dawley (SD) rat (Shin et al., 2007). Research indicated that RBX in a high dose could bring about a toxic effect (Zhang et al., 2013), and the main toxicity of RBX was irritation, which was similar to the inflammatory response (Li et al., 2010). Hence, the clinician mainly uses the processed BX (PBX), especially in the preparations containing *Pinelliae Rhizoma*, which is recorded in the Chinese Pharmacopoeia (2015 edition). Safety is the first considered factor in drug utilization, and the toxicities of RBX and PBX are different (Shin et al., 2007; Wu, Ji, Qiu, & Ye, 2001). The underlying mechanisms of herb processing were the changes of related compositions or active components in the herbs (Cai & Gong, 2009). It is greatly significant to screen out the changed chemical markers, which could be used for quality control and clinical safety use of raw and processed herbs. Thus, it is necessary to study the discrimination of the toxic ingredients between RBX and PBX (Wang et al., 2010).

* Corresponding author.
E-mail address: uabcv@163.com (C. Jin).

https://doi.org/10.1016/j.chmed.2019.03.007
1674-6384/

Ultra performance liquid chromatography-quadrupole time-of-flight mass spectrometry (UPLC/Q-TOF-MS/MS) is a newly developed technique. UPLC has the features to enhance the reproducibility of retention time and increase the chromatographic resolution, sensitivity, and operation speed (Mona, Nathan, Larry, & Daniel, 2005). UPLC/Q-TOF-MS/MS is also a powerful tool for the metabolomics studies (Brown et al., 2009; Gosettia, Chiuminatto, Mazzucco, Mastroianni, & Marengo, 2015; Guy, Tavazzi, Bruce, Ramadan, & Kochhar, 2008). The precise mass values of TOF-MS produced by empirical formulae can infer organic structure accurately at the error less than 5×10^{-6} (Chan et al., 2007). In recent years, H (U) PLC-DAD-TOF-MS has been increasingly used for finding the discrimination of the ingredient between raw and processed medicinal herbs with multivariate statistical analysis (Geng et al., 2013; Liang et al., 2013; Shan et al., 2014).

In this study, samples of the raw and processed BX were analyzed by UPLC/Q-TOF-MS/MS. Then Principal component analysis (PCA) and T-test analysis were adopted to investigate the discrimination between the two groups, and the chemical markers were identified accordingly. These chemical markers were helpful in explaining the mechanism of detoxification of PBX.

2. Materials and methods

2.1. Chemicals and reagents

BX was purchased from the Chinese Medicinal Materials Company (Beijing, China) and identified by associate professor Ke-zhong Deng from Jiangxi University of Traditional Chinese Medicine. The PBX was processed by the method of Fabanxia in Chinese Pharmacopoeia (2015 edition) with the same growing area and collecting time with RBX in the lab, and it was up to standard for detecting of the method of Fabanxia in Chinese Pharmacopoeia (2015 Edition). Acetonitrile (HPLC grade) was purchased from the Tedia Company (USA). Deionized water was purified by Milli-Q system (Millipore, Bedford, MA, USA). Formic acid (HPLC grade) was purchased from Dikma Technology Inc. (Lake Forest, CA, USA).

2.2. Sample preparation

The powder of RBX and PBX were accurately weighed (2.0 g) and ultrasonic-extracted with 50.0 mL of ethanol for 60 min, respectively. The decoctions were filtered through three layers of gauze, and 40.0 mL ethanol were then added for the second decoction with a duration of 30 min. The 16 samples were prepared by the same methods and divided into two groups, the raw BX group and the processed BX group. The samples were concentrated to 10 mL. The resulting solutions were centrifuged at 4000 r/min, the supernatant was filtered through a 0.22 μm membrane, and an aliquot (10 μL) of each filtrate was subjected to UPLC-MS analysis.

2.3. UPLC/Q-TOF-MS/MS measurements

The controls and samples were analyzed on a triple TOF™5600 + MS/MS system (AB SCIEX, Canada) coupled to a Prominence™ UPLC system (Shimadzu, Japan). The UPLC system consisted of a LC-30AD solvent delivery system, SIL-30AC autosampler, CTO-30AC column oven, DGU-20A3 degasser, and CBM-20A controller from Shimadzu (Kyoto, Japan). Separations were accomplished on a Shim-pack xR-ODS III column (2.1 × 75 mm, 1.6 μm). The column oven was maintained at 30 °C.

The mass spectrometer was operated in the positive ESI mode with a DuoSpray™ source (AB SCIEX, Canada), and the mass range was set at *m/z* 100–1500. The parameter settings were used as follow: ion spray voltage: +4500 V; ion source heater: 600 °C; curtain gas: 30 psi; nebulizing gas (GS1), 50 psi; and TIS gas (GS2), 30 psi. For the TOF-MS-IDA (data-independent acquisition)-MS/MS analysis, TOF/MS, the survey scan, and MS/MS experiments were run with 200 ms of accumulation time for TOF/MS and 100 ms of accumulation time in MS/MS experiments. The declustering potential (DP) was set at 120 V. Collision energy (CE) was 30 eV and collision energy spread (CES) was 25 eV in MS/MS experiment. Exploring and interpreting mass spectral data with special tools was carried out for processing accurate mass data and structural elucidation. The sample data were processed by Analyst TF 1.6, while Markerview 1.2.1 and Peakview software (AB SCIEX, Foster City, CA) were employed for data extraction before chemometrics analyzes and quantification of samples, respectively.

The mobile phase A was composed of 0.1% formic acid in water (volume percent), and mobile phase B was acetonitrile. The gradient program of mobile phase was carried out as follows: 0–1.5 min, 10%–10% B; 1.5–20 min, 10%–45% B; 20–25 min, 45%–55% B; 25–35 min, 55%–65% B; 35–38 min, 65%–70% B, 38–40 min, 70%–99% B; 40–43 min, 99%–99% B; 43–45 min, 10%–10% B. The flow rate was 0.25 mL/min and the injection volume was 10 μL.

2.4. Multivariate data processing

The retention time and chromatographic peaks of samples after collecting the original chromatogram by Analyst TF 1.6 was observed. The following parameters were used to identify the peaks from the raw data: subtraction offset was 10 scans; Subtraction multiplication factor was 1.3; The minimum retention time was 0.50 min, the maximum retention time was 45.00 min; Noise threshold was 1000; Minimum retention time peak width was 5 scans; Minimum spectral peak width was 10×10^{-6}; Retention time tolerance was 0.40 min; Mass tolerance was 5.0×10^{-6}, and maximum number of peaks was 5000. These settings allowed the program to find small and narrow mass peaks that can be merged during alignment. The resulting data comprising of peak number (t_R-*m/z* pair), sample name and normalized ion intensity were analyzed by unsupervised PCA and T-test using Markerview 1.2.1 software. The chemical markers were identified by MS/MS fragments and the reference or database of Peakview 1.2.0.3.

3. Results and discussion

3.1. UPLC/Q-TOF-MS/MS analysis of BX samples

The constituents of BX mainly consisted of alkaloids, volatile oils, organic acids, amino acids and protein (Wang, Wu, Ma, & Shi, 2008). It was a challenge to simultaneously determine the different types of bioactive components in the same run using chromatographic analysis due to their differences in polarity. Under the optimized chromatographic and MS conditions, the major components in BX were well separated and detected within 45 min. The representative positive base peak intensity chromatograms (BPC) of raw and processed BX extracts were shown in Fig. 1.

3.2. Multivariate statistical analysis and characteristic markers explored by principal component analysis and T-test analysis

As shown in Fig. 2A, the samples of the RBX and PBX could be distinguished for the aggregation and dispersion of the samples.

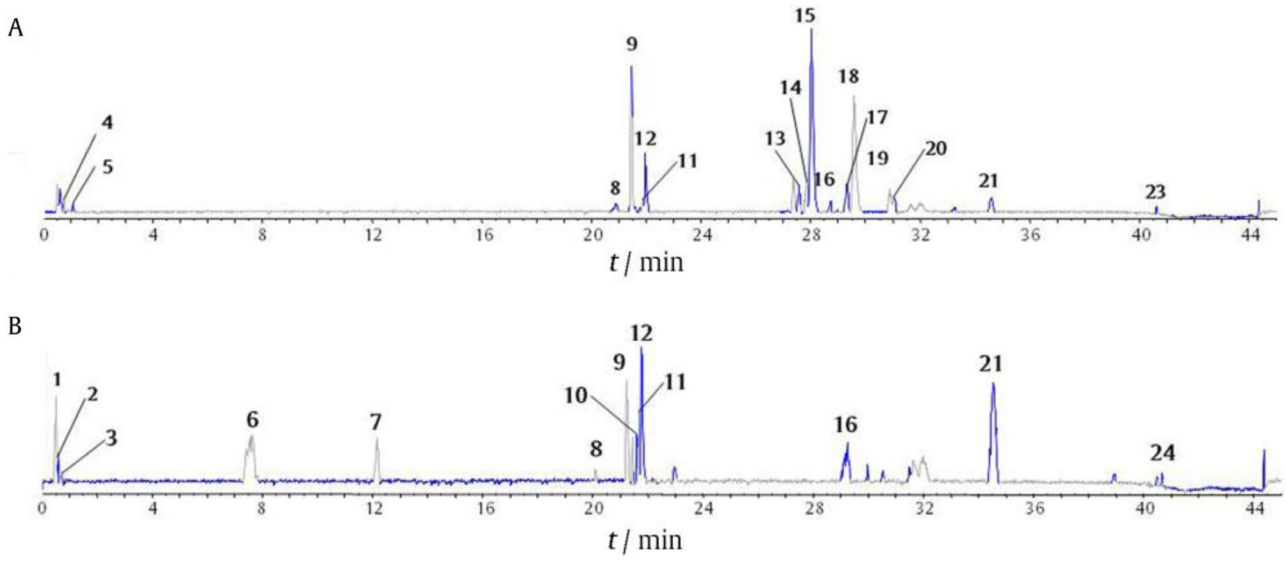

Fig. 1. Base peak intensity chromatograms of RBX (A) and PBX (B) (Peak numbers represented same meanings as Table 1).

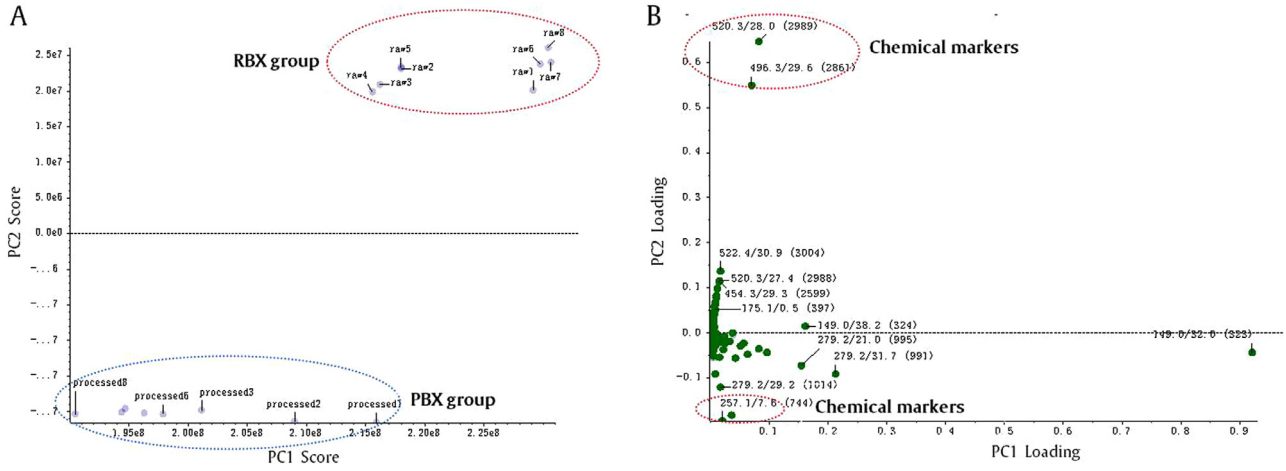

Fig. 2. Scores (A) and loading (B) plots of first two PCs. Dashed line in separated RBX group and PBX group.

It could be seen that the PCA model established in this experiment was well clustered. The loading plot of the PCA could reflect the contribution of the variable to the principal components. The greater the distance from the origin to the principal component was, the greater the contribution to the principal component was. From the loading plot in Fig. 2B, most of the compounds were clustered together, the difference point of "outliers" were the chemical markers of in two groups, the farther the distance was away from the zero, the greater the difference was. The *m/z* 520, *m/z* 496, and *m/z* 257 were the farthest ion.

However, in this way, it was still not possible to distinguish the components from PCA. Therefore, 16 samples were added to the dataset and carried out again on the final dataset by the T-test. Log (fold change) versus *P*-value for the raw BX group and processed BX group were shown in Fig. 3. Combined with the difference value of load chart, the chemical markers with larger contribution to classification were screened out under the two modes.

Those compositions were chosen as chemical markers with fold change more than 2.5 and *P*-value less than 0.05 in Fig. 3. Specific data of chemical markers were shown in Table 1.

3.3. Identifying chemical markers

To further assess the BX-induced biochemical changes, we tried to identify the chemical marker obtained from the compared samples. For lacking reference standards, the identification was realized by comparing the accurately measured mass value and MS/MS fragments with the reference or database. The detailed data were shown in Table 1. The structures of some discrimination ingredients between two groups were shown in Fig. 4. As the graph showed, those chemical markers had significant differences between two groups.

The protonated molecule of Peak **7** at *m/z* 257.0815 exhibited the identical mass-to-charge ratio value as the fragment ion $[M+H-162]^+$ derived from Peak **6**, suggesting that Peak **7** might be aglycone of Peak **6**. The alycone ion at *m/z* 257.0815 could be further fragmented to the product ion at *m/z* 135.0086 or 119.0502 through RDA cleavage. Based on the above information, Peaks **6** and **7** were tentatively identified as liquiritin and liquiritigenin (Zhang et al., 2013). The liquiritin and liquiritigenin appeared in the PBX group, but did not appear in the RBX group.

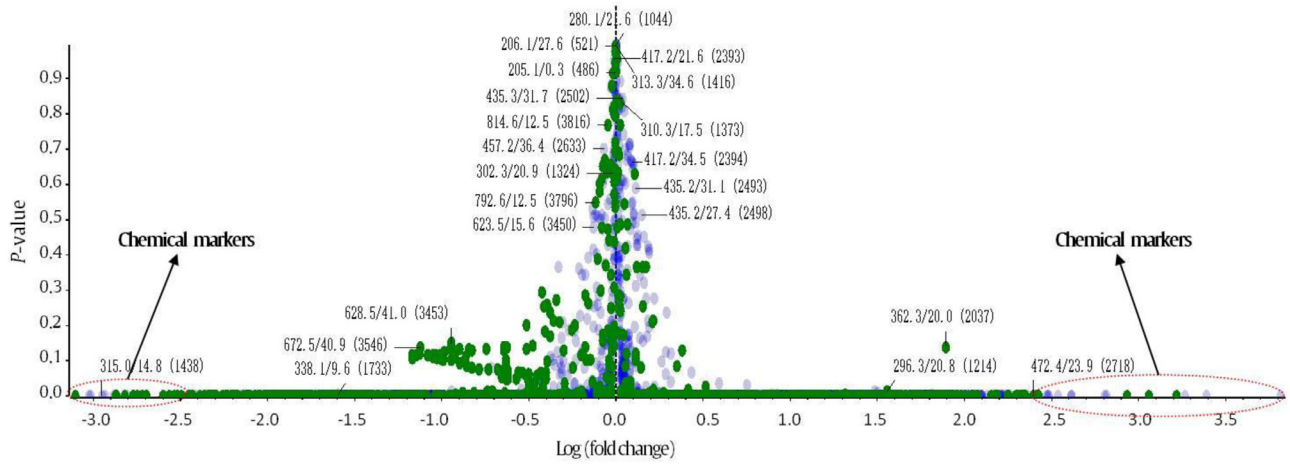

Fig. 3. Log (fold change) versus *P*-value for RBX group and PBX group.

According to the relevant data (Yan et al., 2013), the chemical marker at *m/z* 520.3377 were identified as LPC (18: 2) (Peak **15**), and the marker at *m/z* 496.3379 and 522.3554 were identified as LPC (16:1) (Peak **18**) and LPC (18:1) (Peak **19**) respectively. We selected *m/z* 520.3377 to illustrate the chemical marker identification process. In positive ion spectrum (Fig. 5), the parent ion $[M+H]^+$ at *m/z* 520.3377 was found. Another two high-abundance fragment ions at *m/z* 184.0738 and 104.1078 represent the head group information of phosphatidylcholine class. These two fragment ions represent the fragments of $[H_2O_3PO\text{-}CH_2CH_2N(CH_3)_3]^+$ and $[HOCH_2CH_2N(CH_3)_3]^+$, respectively. The fragment ion at *m/z* 502 $[M+H\text{-}H_2O]^+$ was generated from the loss of H_2O of the ion at *m/z* 520, indicating that the biomarker belonged to lysophosphatidylcholine. Also, Peaks **14** and **17** were identified as 9,12-octadecadienoate and 3-{[(2-aminoethoxy)phosphoryl]oxy}-2-hydroxypropyl palmitate. All LPCs decreased in the processed BX group.

With the same method described above, the other chemical markers were identified. Peaks **11** and **12** were identified as 2-aminooctadec-4–yne-1,3-diol and phytosphingosine, which were sphingosine. Peaks **13, 20**, and **23** were identified as 2,3-dihydroxypropyl-9,12-octadecadienoate-hexose-hexose, 2,3-dihydroxypropyl(9Z,12Z)−9,12-octadecadienoate-hexose and 1-palmitoylglycerol, which were glycerol esters. Peak **21** was identified as linoleoyl ethanolamide. All of them raised in the processed BX group, but the liquiritin, liquiritigenin, and lysophosphatidylcholine (LPC) were rapidly explored as the most characteristic markers in raw BX group and processed BX group.

3.4. Elucidation of chemical marker

Lysophosphatidylcholine (LPC), also called lysolecithin, is an important lipid molecule in mammalian tissues. Accumulation of LPC is associated with a host of diseases such as atherosclerosis, myocardial ischemia, and inflammatory diseases (Quinn, Parthasarathy, & Steinberg, 1988; Sedlis, Hom, Sequeira, & Esposito, 1993; Vidaver, Ting, & Lee, 1985). LPC is also a major lipid constituent and exhibits several types of neuroactivity in the nervous system (Wang, Deems, & Dennis, 1997), and induces neuronal sheaths demyelination, together with a variable degree of axonal degeneration (Hall et al., 1972; Jean, Allamargot, Barthelaix-Pouplard, & Fressinaud, 2002), which is a common pathological characteristic of neurodegenerative diseases (Iqbal et al., 2003; Kostrzewa et al., 2003).

Irritation of BX is similar to the inflammatory response, which is hyperemia, swelling, blister and pain. Powder of BX can increase the permeability of mice capillaries, peritoneal exudates, and the content of prostaglandin E (PGE) in the exudation of inflammatory mediators, and the content of histamine was decreased by intraperitoneal injection (Li et al., 2010). Nanomolar concentrations of LPC can recruit monocytes and induce pro-inflammatory cytokine production in macrophages (Olofsson, Andersson, Nilsson, & Björkbacka, 2008). Also, LPC has been shown to induce both adhesion molecules and chemokine release in cultured endothelial cells (Kume, Cybulsky, & Gimbrone, 1992; Takahara, Kashiwagi, Maegawa, & Shigeta, 1996). LPC can induce cytokine production in human monocytes (IL-1b) and rat aortic smooth muscle cells (MCP-1) (Wu, Hurt-Camejo, & Wiklund, 1998). LPC is linked to the polarization of pro-inflammatory M1 macrophage which characteristically produces pro-inflammatory cytokines, such as IL-12, IL-1b, TNF-α, and IL-6, and plays a crucial role in the initiation and perpetuation of inflammatory response (Qin, Qiu, & Zhao, 2014).

Liquiritin and liquiritigenin are flavonoids from liquorice. Liquiritin attenuates advanced glycation end products (AGE)-induced endothelial dysfunction via the receptor for AGE (RAGE)/nuclear factor-kB (NF-kB) pathway in human umbilical vein endothelial cells (Zhang et al., 2012), and inhibits focal cerebral ischemia/reperfusion in mice via its anti-oxidative and anti-apoptotic properties (Sun et al., 2010). Liquiritigenin also has anti-inflammatory effects against lipopolysaccharide (LPS)-induced production of NF-kB-dependent inducible nitric oxide synthase (iNOS) and pro-inflammatory cytokines in the murine macrophage cell line, Raw264.7 (Kim et al., 2008). Liquiritigenin exerts cytoprotective effects against heavy metal-induced toxicity in rat hepatocyte-derived cultured cells (Kim et al., 2004) and shows protective efficacy in rats with acetaminophen-induced (Kim, Ki, & Lee, 2006) or in mice with galactosamine/olipopoly-saccharide-induced (Kim, Kang, & Lee, 2009) carbon tetrachloride-induced liver injuries (Shimamura, Suzuki, Hanano, Suzuki, & Sugiyama, 1993). Liquiritigenin is now being evaluated in preclinical studies as an oral agent for the treatment of inflammatory liver disease (Kang, Sohn, Baek, Lee, & Lee, 2010). The previous animal study indicated that excessive or long-term use of raw BX would cause liver damage (Yang et al., 1988; Zhang et al., 2011). Therefore, we can see liquiritin and liquiritigenin can reduce the toxicity of liver damage and inflammatory response.

Table 1
MS analytical data of chemical marker ingredients.

Peak No.	t_R / min	Assigned identity	Molecular formula	$[M+H]^-$ *m/z*		Mass accuracy ($\times 10^{-6}$)	Trend	Type	$[M+NH_4]^+$ *m/z*	Ion mass / (*m/z*)
				Mean measured mass/Da	Theoretical exact mass/Da					
1	0.50	Unknown		734.702			↑			604.7928, [M+H-130], 474.8338 [M+H-130-130], 344.8757 [M+H-130-130-130], 214.9172 [M+H-130-130-130-130]
6	7.42	liquiritin	$C_{21}H_{22}O_9$	419.1342	419.1337	1.3	↑	flavone		257.0808 [M+H-162], 239.0714, 147.044, 137.0237
7	12.18	liquiritigenin	$C_{15}H_{12}O_4$	257.0814	257.0808	2.1	↑	flavone		239.0699 [M+H-18], 211.0757 [M+H-18-28], 147.0447
8	20.19	N-[1-hydroxy-2-propanyl]-5,8,11,14-icosatetraenamide	$C_{23}H_{39}NO_2$	362.3048	362.3053	−1.5	↓			344.2943 [M+H-18]
9	21.25	Unknown	$C_{22}H_{37}NO$	332.2939	332.2948	−2.7	↓			314.2828 [M+H-18], 91.0539
10	21.45	N-stearoylethanolamine	$C_{20}H_{41}NO_2$	328.3202	328.3210	−2.5	↑			310.3107 [M+H-18]
11	21.61	2-aminooctadec-4-yne-1,3-diol	$C_{18}H_{35}NO_2$	298.2754	298.2741	4.5	↑	Sphingosine		280.2634 [M+H-18], 250.2530 [M+H-18-30]
12	21.78	phytosphingosine	$C_{18}H_{39}NO_3$	318.2996	318.3003	−2.1	↑	Sphingosine		300.2901 [M+H-18], 282.2795 [M+H-18-18], 270.2785
13	27.59	2,3-dihydroxypropyl-9,12-octadecadienoate-hexose-hexose	$C_{33}H_{58}O_{14}$	679.3877	679.3899	−3.3	↓	Glycerol esters	696.4118	517.3352 [M+H-162], 355.2840 [M+H-162-162], 337.2743 [M+H-162-162-18], 263.2365 [M+H-162-162-18-74], 245.2260 [M+H-162-162-18-74-18], 163.0593
14	27.86	9,12-octadecadienoate	$C_{23}H_{44}NO_7P$	478.2939	478.2928	2.3	↓	LPC		460.2812 [M+H-18], 337.2733 [M+H-18-123], 306.2787 [M+H-18-123-31]
15	28.05	LPC (18:2)	$C_{26}H_{50}NO_7P$	520.3377	520.3377	−3.8	↓	LPC		502.327 [M+H-18], 184.0724, 124.9995, 104.1067
16	29.22	a-linolenic acid	$C_{18}H_{30}O_2$	279.2329	279.2319	3.5	↑			261.2220 [M+H-18], 243.2105 [M+H-18-18], 223.1697 [M+H-18-18-20], 209.1530 [M+H-18-18-20-14], 195.1401 [M+H-18-18-20-14-14], 173.1342 [M+H-18-18-20-14-14-22], 149.0240 [M+H-18-18-20-14-14-22-24]
17	29.34	3-{[(2-aminoethoxy)phosphoryl]oxy}-2-hydroxypropyl palmitate	$C_{21}H_{44}NO_7P$	454.2914	454.2928	−3.1	↓	LPC		436.2814 [M+H-18], 313.2737 [M+H-18-123], 282.2790 [M+H-18-123-31]

(*continued on next page*)

Table 1 (*continued*)

Peak No.	t_R / min	Assigned identity	Molecular formula	$[M+H]^-$ *m/z*		Mass accuracy ($\times 10^{-6}$)	Trend	Type	$[M+NH_4]^+$ *m/z*	Ion mass / (*m/z*)
				Mean measured mass/Da	Theoretical exact mass/Da					
18	29.60	LPC (16:1)	$C_{24}H_{50}NO_7P$	496.3379	496.3398	−3.8	↓	LPC		478.3283 [M+H-18], 313.2742 [M+H-18-165], 258.1102 [M+H-18-165-55], 184.0727, 124.9995, 104.1069
19	30.90	LPC (18:1)	$C_{26}H_{52}NO_7P$	522.3530	522.3554	−4.6	↓	LPC		504.3443 [M+H-18], 184.0730, 124.9997, 104.1068
20	31.05	2,3-dihydroxypropyl(9Z,12Z)-9,12-octadecadienoate-hexose	$C_{27}H_{48}O_9$	517.3353	517.3371	−3.5	↓	Glycerol esters	534.3607	534.3607 [M+NH4], 355.2836 [M+H-162], 337.2730 [M+H-162-18], 263.2368 [M+H-162-18-74], 245.2264 [M+H-162-18-74-18], 95.0858
21	34.55	linoleoyl ethanolamide	$C_{20}H_{37}NO_2$	324.2892	324.2897	−1.6	↑			306.2621 [M+H-18], 245.2275 [M+H-18-61]
22	38.93	Unknown		326.3061			↑			309.2799 [M+H-17]
23	40.62	1-palmitoylglycerol	$C_{19}H_{38}O_4$	331.2841	331.2843	−0.6	↓	Glycerol esters		313.2741 [M+H-18], 239.2366 [M+H-18-74], 95.0853

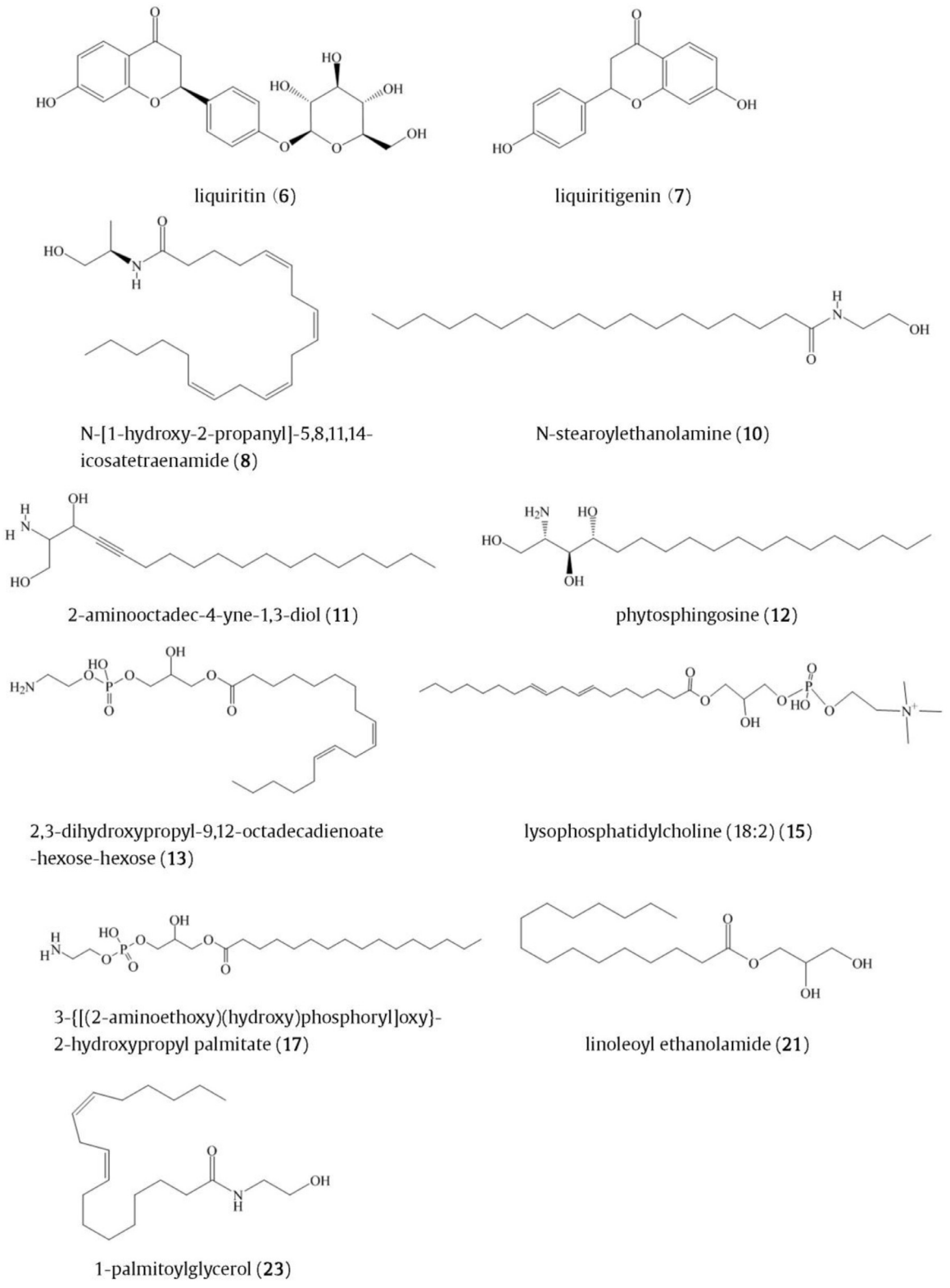

Fig. 4. Structures of chemical marker ingredients in RBX and PBX.

4. Conclusion

Lysophosphatidylcholine (LPC) was first proposed as a toxic component of *P. ternata*. The characteristic ingredient of discrimination, including LPC, liquiritin, and liquiritigenin can reduce the liver damage and inflammatory toxicity of raw BX. An approach to explain mechanisms of reducing the toxicity of medicinal plants by processing using UPLC/Q-TOF-MS/MS coupled with multivariate statistical analysis was proposed. This new approach can avoid replication in isolation, purification, and identification of the identical components in both raw and processed herbs, and therefore, could be a cost-effective way to determine potential chemical

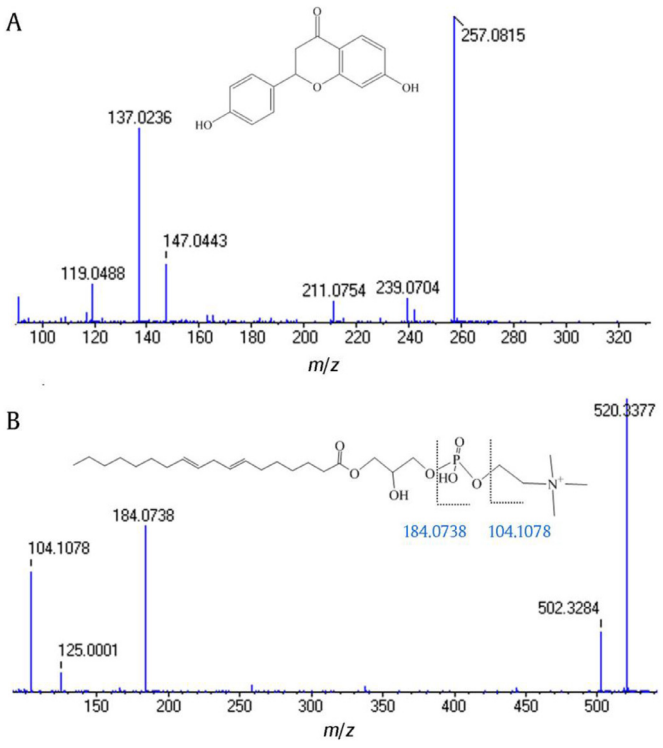

Fig. 5. Mass spectra of ingredients **7** (A) and **15** (B).

markers of processed herbs. Moreover, chemical markers also could be used to differentiate raw from processed herbs for the quality control and safety application in clinical practice.

Conflict of interest

All authors declare that they have no competing interests.

Acknowledgments

This work was supported by the National Natural Science Foundation of China (No. 81460595).

References

Brown, M., Dunn, W. B., Dobson, P., Patel, Y., Winder, C. L., Francis-McIntyre, S., & et al. (2009). Mass spectrometry tools and metabolite-specific databases for-molecular identification in metabolomics. *Analyst, 134*, 1322–1332.

Cai, B. C., & Gong, Q. F. (2009). Processing of Chinese Medicinal Herbs. People Health Press.

Chan, E. C., Yap, S. L., Lau, A. J., Leow, P. C., Toh, D. F., & Koh, H. L. (2007). Ultra-performance liquid chromatography/time-of-flightmass spectrometry based-metabolomics of raw and steamed *Panax notoginseng*. Rapid Communications Mass Spectrometry, *21*, 519–528.

Geng, L. L., Sun, H. Y., Yuan, Y., Liu, Z. Z., Cui, Y., & Bi, K. S. (2013). Discrimination of raw and vinegar-processed *Genkwa Flos* using metabolomics coupled with multivariate data analysis: A discrimination study with metabolomics coupled with PCA. *Fitoterapia, 84*, 286–294.

Gosettia, F., Chiuminatto, U., Mazzucco, E., Mastroianni, R., & Marengo, E. (2015). Ultra-high-performance liquid chromatography/tandem high-resolution mass spectrometry analysis of sixteen red beverages containing carminic acid: Identification of degradation products by using principal component analysis/discriminant analysis. *Food Chemistry, 167*, 454–462.

Guy, P. A., Tavazzi, I., Bruce, S. J., Ramadan, Z., & Kochhar, S. (2008). Globalmetabolic profiling analysis on human urine by UPLC-TOFMS: Issues and method validation in *nutritional metabolomics*. *Journal of Chromatography B, 871*, 253–260.

Hall, S. M. (1972). The effect of injections of lysophosphatidyl choline into white matter of the adult mouse spinal cord. *Journal of Cell Science, 10*, 535–546.

Iqbal, K., Alonso, C., ElAkkad, E., Gong, C. X., Haque, N., Khatoon, S., & et al. (2003). Alzheimer neurofibrillary degeneration: Therapeutic targets and high throughput assays. *Journal of Molecular Neuroscience, 20*, 425–429.

Jean, I., Allamargot, C., Barthelaix-Pouplard, A., & Fressinaud, C. (2002). Axonal lesions and PDGF-enhanced remyelination in the rat corpus callosum after lysolecithin demyelination. *Neuroreport, 13*, 627–631.

Jin, S. Y., & Wang, Q. (2004). Studies on Processing of Chinese Medicinal Yinpian and Its Clinical Application. Press of Chemistry Industry.

Kang, H. E., Sohn, S. I., Baek, S. R., Lee, J. W., & Lee, M. G. (2010). Liquiritigenin pharmacokinetics in a rat model of diabetes mellitus induced by streptozotocin: Greater formation of glucuronides in the liver, especially M2, due to increased hepatic uridine 5-diphosphoglucuronic acid level. *Metabolism Clinical and Experimental, 59*, 1472–1480.

Kim, S. C., Bun, S. H., Yang, C. H., Kim, C. Y., Kim, J. W., & Kim, S. G. (2004). Cytoprotective effects of *Glycyrrhizae Radix* extract and its active component liquiritigenin against cadmium-induced toxicity (effects on bad translocation and cytochrome c-mediated PARP cleavage). *Toxicology, 197*, 239–251.

Kim, Y. W., Ki, S. H., & Lee, J. R. (2006). Liquiritigenin, an aglycone of liquiritin in *Glycyrrhizae Radix*, prevents acute liver injuries in rats induced by acetaminophen with or without buthionine sulfoximine. *Chemico-biological Interactions, 161*, 125–138.

Kim, Y. W., Kang, H. E., & Lee, M. G. (2009). Liquiritigenin, a flavonoid aglycone from licorice, has a choleretic effect and the ability to induce hepatic transporters and phase-II enzymes. American Journal of Physiology-Gastrointestinal Liver Physiology, *296*, G372–G381.

Kim, Y. W., Zhao, R. J., Park, S. J., Lee, J. R., Cho, I. J., & Yang, C. H. (2008). Anti-inflammatory effects of liquiritigenin as a consequence of the inhibition of NF-kappaB-dependent iNOS and proinflammatory cytokines production. *British Journal of Pharmacology, 154*, 165–173.

Kostrzewa, R. M., & Segura-Aguilar, J. (2003). Novel mechanisms and approaches in the study of neurodegeneration and neuroprotection. A review. Neurotoxicity Research, *5*, 375–383.

Kume, N., Cybulsky, M. I., & Gimbrone, M. A. (1992). Lysophosphatidylcholine, a component of atherogenic lipoproteins, induces mononuclear leukocyte adhesion molecules in cultured human and rabbit arterial endothelial cells. *Journal of Clinical Investigation, 90*, 1138–1144.

Li, S. L., Song, J. Z., Qiao, C. F., Zhou, Y., Qian, K., & Lee, K. (2010). A novel strategy to rapidly explore potential chemical markers for the discrimination between raw and processed *Radix Rehmanniae* by UHPLC-TOFMS with multivariate statistical analysis. *Journal of Pharmaceutical and Biomedical Analysis, 51*, 812–823.

Liang, Q. D., Ma, J., Ma, Z. C., Wang, Y. G., Tan, H. L., Xiao, C. R., & et al. (2013). Chemical comparison of dried rehmannia root and prepared rehmannia root by UPLC-TOF MS and HPLC-ELSD with multivariate statistical analysis. *Acta Pharmaceutica Sinica B, 3*, 55–64.

Mona, I. C., Nathan, C. T., Larry, R. M., & Daniel, R. D. (2005). Improving LC–MS sensitivity through increases in chromatographic performance: Comparisons of UPLC–ES/MS/MS to HPLC-ES/MS/MS. *Journal of Chromatography B, 825*, 134–143.

Olofsson, K. E., Andersson, L., Nilsson, J., & Björkbacka, H. (2008). Nanomolar concentrations of lysophosphatidylcholine recruit monocytes and induce pro-inflammatory cytokine production in macrophages. *Biochemical and Biophysical Research Communications, 370*, 348–352.

Qin, X. F., Qiu, C. G., & Zhao, L. S. (2014). Lysophosphatidylcholine perpetuates macrophage polarization toward classically activated phenotype in inflammation. *Cellular Immunology, 289*, 185–190.

Quinn, M. T., Parthasarathy, S., & Steinberg, D. (1988). Lysophosphatidylcholine: A chemotactic factor for human monocytes and its potential role in atherogenesis. *Proceedings of the National Academy of Sciences of the United States of America, 85*, 2805–2809.

Sedlis, S. P., Hom, M., Sequeira, J. M., & Esposito, R. (1993). Lysophosphatidyl choline accumulation in ischemic human myocardium. *Journal of Laboratory and Clinical Medicine, 121*, 111–117.

Shan, G. S., Zhang, L. X., Zhao, Q. M., Xiao, H. B., Zhuo, R. J., Xu, G., & et al. (2014). Metabolomic study of raw and processed atractylodes macrocephala Koidz by LC-MS. *Journal of Pharmaceutical and Biomedical Analysis, 98*, 74–84.

Shimamura, H., Suzuki, H., Hanano, M., Suzuki, A., & Sugiyama, Y. (1993). Identification of tissues responsible for the conjugative metabolism of liquiritigenin in rats: An analysis based on metabolite kinetics. *Biological & Pharmaceutical Bulletin, 6*, 899–907.

Shin, S. H., Park, D. S., Jeon, J. H., Nam, S. Y., Yun, Y. W., & Kam, Y. B. (2007). Effect of *Pinellia ternata* extract on fetal development of rats. *Reproductive Toxicology, 24*, 57–80.

Sun, Y. X., Tang, Y., Wu, A. L., Liu, T., Dai, X. L., & Zheng, Q. S. (2010). Neuroprotective effect of liquiritin against focal cerebral ischemia/reperfusion in mice via its antioxidant and antiapoptosis properties. *Journal of Asian Natural Products Research, 12*, 1051–1060.

Takahara, N., Kashiwagi, A., Maegawa, H., & Shigeta, Y. (1996). Lysophosphatidylcholine stimulates the expressionand production of MCP-1 by human vascular endothelial cells. *Metabolism, 45*, 559–564.

Vidaver, G. A., Ting, A., & Lee, J. W. (1985). Evidence that lysolecithin is an important causal agent of atherosclerosis. *Journal of Theoretical Biology, 115*, 27–41.

Wang, A., Deems, R. A., & Dennis, E. A. (1997). Cloning, expression, and catalytic mechanism of murine lysophospholipase I. *The Journal of Biological Chemistry, 272*, 12723–12729.

Wang, J. (2010). The reducing toxicity of *Pinellia ternata* (Thunb.). *Shanxi Journal of Traditional Chinese Medicine, 31*, 1299 -1231.

Wang, X. S., Wu, Y. F., Ma, J. Y., & Shi, Q. L. (2008). Study on chemical components and pharmacological activities of *Pinellia ternate*. Qilu Pharmaceutical Affairs, *27*, 101–103.

Wu, H., Ji, R., Qiu, L. Y., & Ye, D. J. (2001). Studies on quantification indexes in stimulation of raw *Rhizoma Pinellia*. *Chinese Traditional Patent Medicine, 22*, 419–421.

Wu, Y. L., Hurt-Camejo, E., & Wiklund, O. (1998). Lysophosphatidylcholine induces the production of IL-1beta by human monocytes. *Atherosclerosis, 137*, 351–357.

Yang, S. Y., Ye, W. H., & Wu, Z. L. (1988). The study on acute toxicity, subacute toxicity and accumulative toxicity induced by processed and unprocessed *Pinellia ternate*. *Zhongchengyao, 7*, 18–19.

Yan, Y., Chai, C. Z., Wang, D. W., Yue, X. Y., Zhu, D. N., & Yu, B. Y. (2013). HPLC–DAD-Q-TOF-MS/MS analysis and HPLC quantitation of chemical constituents in traditional Chinese medicinal formula Gegen Decoction. *Journal of Pharmaceutical and Biomedical Analysis, 80*, 192–202.

Ye, D. J., & Yuan, S. T. (2005). Dictionary of Chinese Herbal Processing Science. Shanghai Science and Technology Press.

Zhang, X., Song, Y., Han, X., Feng, L., Wang, R., & Zhang, M. (2012). Liquiritin attenuates advancedglycation end products-induced endothelial dysfunction via RAGE/NF-kB pathway in human umbilical vein endothelial cells. Molecular and Cell Biochemistry, *374*, 191–201.

Zhang, Y. N., Huang, Y. Y., & Bao, Z. Y. (2011). Experimental study on the dosage–time-toxicity relationship of acute hepatotoxicity induced by percolation liquid of acid from *Rhizoma Pinelliae* in mice. *Chinese Journal of Pharmacovigilance, 8*, 15–19.

Zhang, Z. H., Zhao, Y. Y., Cheng, X. L., Dai, Z., Zhou, C., & Bai, X. (2013). General toxicity of *Pinellia ternata* (Thunb.) Berit. in rat: A metabonomic method for profiling of serum metabolic changes. *Journal of Ethnopharmacology, 149*, 303–310.

Zhang, Z. H., Zhao, Y. Y., Cheng, X. L., Lin, R. C., Dai, Z., & Zhou, C. (2013). Metabonomic study of biochemical changes in the rat urine induced by *Pinellia ternata* (Thunb.) Berit. *Journal of Pharmaceutical and Biomedical Analysis, 85*, 186–193.